

# Experimental demonstration of higher-order Laguerre–Gauss mode interferometry

Paul Fulda,<sup>1</sup> Keiko Kokeyama,<sup>1</sup> Simon Chelkowski,<sup>1</sup> and Andreas Freise<sup>1</sup>

<sup>1</sup>*School of Physics and Astronomy, University of Birmingham, Edgbaston, Birmingham B15 2TT, UK*

(Dated: June 16, 2022)

The compatibility of higher-order Laguerre–Gauss (LG) modes with interferometric technologies commonly used in gravitational wave detectors is investigated. In this paper we present the first experimental results concerning the performance of the LG<sub>33</sub> mode in optical resonators. We show that the Pound-Drever-Hall error signal for a LG<sub>33</sub> mode in a linear optical resonator is identical to that of the more commonly used LG<sub>00</sub> mode, and demonstrate the feedback control of the resonator with a LG<sub>33</sub> mode. We succeeded to increase the mode purity of a LG<sub>33</sub> mode generated using a spatial-light modulator from 51% to 99% upon transmission through a linear optical resonator. We further report the experimental verification that a triangular optical resonator does not transmit helical LG modes.

PACS numbers: 04.80.Nn, 95.75.Kk, 42.50.Tx, 95.55.Ym

## I. INTRODUCTION

The sensitivity of future gravitational wave detectors will be limited by the thermal noises of the test masses, and much of the work within the gravitational wave community is currently aimed at reducing the effects of this noise. One proposed method for thermal noise reduction is to use a higher-order Laguerre–Gauss (LG) beam in the main interferometer, in place of the currently standard fundamental LG<sub>00</sub> beam [1]. Higher-order LG modes provide wider intensity distributions for the same optical losses and can therefore average better over the mirror surface distortions caused by the thermal motions [2]. Some of us recently showed that the potential detection rate of binary neutron star inspiral systems with the Advanced Virgo detector could be increased by a factor of 2.1 if the LG<sub>33</sub> beam was used in place of the LG<sub>00</sub> beam [3]. In addition to the thermal noise benefits, the wider intensity distributions of higher-order LG beams have been shown to reduce the magnitude of thermal aberrations of optics within the interferometers [2]. This would reduce the extent to which thermal compensation systems are relied upon in future detectors to reach design sensitivity.

An investigation using numerical simulations, into the sensing and control signals for length and alignment with a LG<sub>33</sub> beam in advanced detectors also yielded positive results, indicating that the LG<sub>33</sub> beam performed as well if not better than the LG<sub>00</sub> beam in all of the examined criteria [3]. We present the results of an experimental follow-on study into the interferometric performance of higher-order LG beams, in order to assess how much of the potential for sensitivity improvement is realizable in practice. The first crucial test for the interferometric performance of LG<sub>33</sub> modes is their compatibility with mode cleaner technology. We show that the mode cleaner effect works equivalently for the LG<sub>33</sub> mode as for the LG<sub>00</sub> mode in a linear optical resonator as depicted in figure 1. We also demonstrate the non-compatibility of helical LG modes with three mirror mode cleaners.

## II. PERFORMANCE OF HIGHER-ORDER LAGUERRE–GAUSS BEAMS IN MODE CLEANER CAVITIES

Laguerre–Gauss modes represent a complete set of solutions to the paraxial wave equation, and as such are well suited to modeling the eigenmodes of spherical optical resonators [4]. There is some lack of consensus in current literature about the exact naming of LG mode functions. Much of the literature relating to higher-order LG modes refers to modes with spiral phase fronts, which carry orbital angular momenta  $l\hbar$  per photon, where  $l$  is the azimuthal mode index [5–7]. Equation 1 shows the normalized form of the complex amplitude of this mode set, which in the following will be referred to as *helical* LG modes.

$$u_{p,l}^{\text{hel}}(r, \phi, z) = \frac{1}{w(z)} \sqrt{\frac{2p!}{\pi(|l|+p)!}} e^{i(2p+|l|+1)\Psi(z)} \times \left(\frac{\sqrt{2}r}{w(z)}\right)^{|l|} L_p^{(|l|)}\left(\frac{2r^2}{w(z)^2}\right) e^{-ik\frac{r^2}{2q(z)}+il\phi} \quad (1)$$

with  $p \geq 0$  the radial mode index and  $l$  the azimuthal mode index. The other parameters in this equation, as well as those in equation 2, have their usual meaning, see, for example [8]. An alternative form of LG modes with a sinusoidal amplitude dependence in azimuthal angle can be used equally well. The normalized form of the complex amplitude of this mode set is shown in equation 2; we will refer to this mode set as *sinusoidal* LG modes.

$$u_{p,l}^{\text{sin}}(r, \phi, z) = \frac{2}{w(z)} \sqrt{\frac{2p!}{1+\delta_{0l}\pi(|l|+p)!}} e^{i(2p+|l|+1)\Psi(z)} \times \left(\frac{\sqrt{2}r}{w(z)}\right)^{|l|} L_p^{(|l|)}\left(\frac{2r^2}{w(z)^2}\right) e^{-ik\frac{r^2}{2q(z)}} \left\{ \begin{array}{l} \sin(l\phi) \\ \cos(l\phi) \end{array} \right\}. \quad (2)$$

A complete set of sinusoidal solutions consists of the functions as given in equation 2 using  $\cos(l\phi)$  for  $l \geq 0$  and

$\sin(l\phi)$  if  $l < 0$ . Higher-order LG modes of both sets offer improvements in thermal noise for gravitational wave interferometers compared to the  $\text{LG}_{00}$  mode, however the advantage is greater for the helical modes than for the sinusoidal modes [2].

A number of different methods for generating higher-order LG modes have been demonstrated [7]. However, so far the optimization of higher-order LG beam sources has largely been in a different direction to that which is required by the gravitational wave detector community. For example the use of LG beams in the cold atoms and optics fields often requires high-speed manipulation of the beam parameters and positions, whereas the use of LG modes in high-precision interferometry depends on mode purity and stability. One of the leading candidate methods for the latter is the use of diffractive optics, or *phase plates* for conversion from a  $\text{LG}_{00}$  mode to a higher-order LG mode, due to their stability, as well as potentially high conversion efficiency and output mode purity. Other conversion methods include using computer generated holograms [9], spatial light modulators [10] and astigmatic mode converters [6]. However, none of these mode conversion methods are perfect, and some light inevitably remains in unwanted modes. An effectively pure and stable higher-order LG mode light source for gravitational wave interferometers can possibly be achieved with the implementation of *mode cleaner cavities*.

In practice, mode cleaners take the form of medium-to high-finesse optical resonators which are feedback controlled to remain on resonance for a chosen laser mode [11]. Mode cleaners are used in several locations in gravitational wave interferometers. So-called *pre-mode cleaners* are used in the initial frequency stabilization chain of the laser. These typically employ small, monolithic spacers in air. The beam then passes the *input mode cleaners*, suspended optical cavities in vacuum whose main function is to filter beam geometry fluctuations (also called beam-jitter noise). Modern laser interferometers also include optical cavities in the main interferometer, which act as additional mode cleaning cavities. Often a small in-vacuum output mode cleaner is then used to filter the light leaving the interferometer before it reaches the photo detectors. Mode cleaners can in principle be used to increase the spatial mode purity of any Gaussian mode. Experimental verification of the compatibility of higher-order LG beams with mode cleaner technology is of paramount importance for determining the future prospects for LG beams in gravitational wave interferometers.

Currently a triangular arrangement is favored for the mode cleaners in gravitational wave detectors as it allows to spatially separate the injected beam from the reflected beam, enabling a length control error signal to be measured in reflection without the need for polarizing optics. However, triangular cavities are not ideal for use with higher-order modes for two reasons:

Mode cleaner	Finesse	FSR	TEM <sub>01</sub> suppression	Throughput
GEO MC1 [12]	2700	37.48 MHz	1325	80 %
GEO MC2 [12]	1900	37.12 MHz	937	72 %
Virgo IMC [13]	1181	1.044 MHz	NA	86.6 %
Linear MC	172	714 MHz	50.1	63 %
Triangular MC	300	714 MHz	87.6	99 %

Table I: Input mode cleaner parameters for some current gravitational wave detectors, as well as those used in this work. TEM<sub>01</sub> suppression factors and throughput percentages are given in terms of light power. The finesse and TEM<sub>01</sub> suppression factors of the mode cleaners used in this work were chosen to be lower than those of the large-scale mode cleaners.

- Helical LG modes cannot be passed through a triangular mode cleaner, as is explained in section III B.
- Any triangular mode cleaner features a spherically curved mirror which is probed by the circulating beam under an angle (not normal incidence). This results in a breaking of the symmetry about the azimuthal angle for the mode cleaner eigenmodes. For this reason, higher-order LG modes are not eigenmodes of triangular mode cleaner cavities [14].

As a result of these considerations, the main experimental setup described here makes use of a linear mode cleaner cavity instead of a triangular cavity. We have however also experimentally verified the non-transmission of helical modes through a triangular cavity (see section III B). The finesse of the linear cavity was chosen to be low in comparison with current detector input mode cleaners in table I. While higher finesse cavities can give a stronger suppression of misalignment modes, it is interesting to see the large improvement that can already be gained through the use of a low-finesse mode cleaner.

### III. LABORATORY DEMONSTRATION

In order to investigate the interferometric performance of the  $\text{LG}_{33}$  beam in a laboratory, it was necessary to produce a reasonably pure example of such a beam. We used a computer-controlled liquid-crystal-on-silicon spatial light modulator (SLM) for LG beam preparation, as demonstrated in [10], because of the availability and adaptability of such devices. We expect the SLM to be replaced by a passive, etched phaseplate in eventual implementations of  $\text{LG}_{33}$  modes in gravitational wave detectors.

The report on the laboratory investigation is comprised of two parts; the first concerning the performance of the sinusoidal and helical  $\text{LG}_{33}$  beams in a linear mode cleaner, and the second concerning specifically the performance of the helical  $\text{LG}_{33}$  beam in a triangular mode

cleaner.

### A. LG mode performance in a linear mode cleaner

The experimental setup for the investigation into the performance of the  $LG_{33}$  mode in a linear mode cleaner is shown in figure 1. The 1064 nm laser light is passed through quarter and half wave plates to set the polarization vector to the optimum orientation for use with the SLM. An electro-optic modulator (EOM) is used to imprint a 15 MHz modulation on the light to enable length control of the mode cleaner with the Pound-Drever-Hall (PDH) method [15]. The light is then reflected from the modulating surface of the SLM, where the phase characteristics of the desired LG mode are imprinted on the beam. The resulting beam is then passed through a telescope to match the beam to the mode cleaner eigenmode.

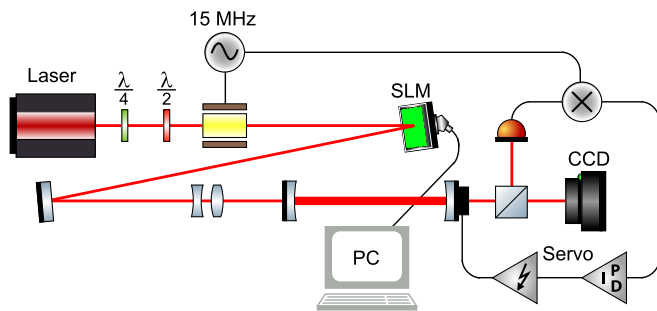


Figure 1: The experimental setup for mode cleaning a SLM generated higher-order LG beam. The  $LG_{00}$  input beam is converted to a higher-order LG beam by the SLM. The resulting beam is passed through a mode-matching telescope into the linear cavity. The transmitted light is used to generate an error signal which is fed back to the PZT attached to the curved end mirror to control the length of the cavity. The transmitted beam is simultaneously imaged on the CCD camera.

The light transmitted through the mode cleaner is passed through a beam splitter, and analyzed at the two ports with a CCD camera and a photodiode respectively. The signal from the photodiode is mixed down with the 15 MHz signal to generate the PDH error signal, which is then fed back to a Piezo-electric transducer (PZT) attached to the mode cleaner end mirror, via a servo and high-voltage amplifier. In this way the length of the mode cleaner cavity can be controlled to maintain the resonance condition for a given mode order. In typical implementations of mode cleaners in gravitational wave interferometers, the error signal is taken in reflection. For this work, however, the mode cleaner cavity was of a low enough finesse to allow the error signal to be taken in transmission.

The PDH error signal for a sinusoidal  $LG_{33}$  input beam is shown in figure 2. This signal was recorded from the output of the mixer while scanning over the  $LG_{33}$  res-

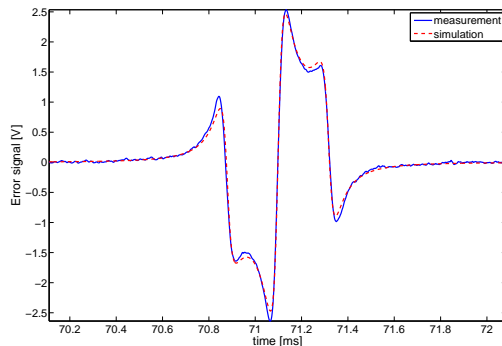


Figure 2: The blue trace shows the PDH error signal from the linear cavity, set up as shown in figure 1, with a sinusoidal  $LG_{33}$  input beam. The red dashed trace shows the PDH error signal for the same optical setup as simulated in the frequency domain simulation software Finesse [16]. While there are small discrepancies between the two traces, the primary features are identical, as predicted in [3].

onance of the linear mode cleaner. The error signal is equivalent to that generated when the input beam is a  $LG_{00}$  beam, confirming the result in [3], and thus allowed a robust feedback control of the cavity length. This is a significant result, as the PDH control loop method is a fundamental technique in the operation of gravitational wave interferometers.

The CCD camera was used to record intensity images of the transmitted beams while the mode cleaner was controlled to be resonant for the  $LG_{33}$  mode. Figure 3 shows the input and output beam intensity patterns for both helical and sinusoidal  $LG_{33}$  beams. The images indicate that the output modes are more symmetrical, and have a higher intensity in the innermost bright radial fringe relative to the others; a feature that is characteristic of  $LG_{33}$  modes. The typical method for measuring the output mode purity would be to pass the output beam through another cavity and observe the magnitudes of different mode order resonances [17]. This method in its original form is not ideal for the work described in this paper however, since in this case the performance of the mode in a cavity is itself being investigated. Instead, we have been able to estimate the mode content based on the intensity pattern alone using numerical simulations. The light transmitted through the cavity can be described well using eigenmodes of said cavity. We were able to construct a numerical model representing the the measured intensity pattern as a sum of LG eigenmodes using the following steps. We initially performed non-linear fits of the  $LG_{33}$  eigenmode to the measured intensity patterns. Figure 4 shows the residuals of such fits: the left panel shows the residual between the input sinusoidal  $LG_{33}$  beam intensity pattern shown in figure 3 and a best-fit theoretical  $LG_{33}$  mode. The central panel shows the equivalent residual for the output sinusoidal  $LG_{33}$  beam intensity pattern. It can be seen that the scale of

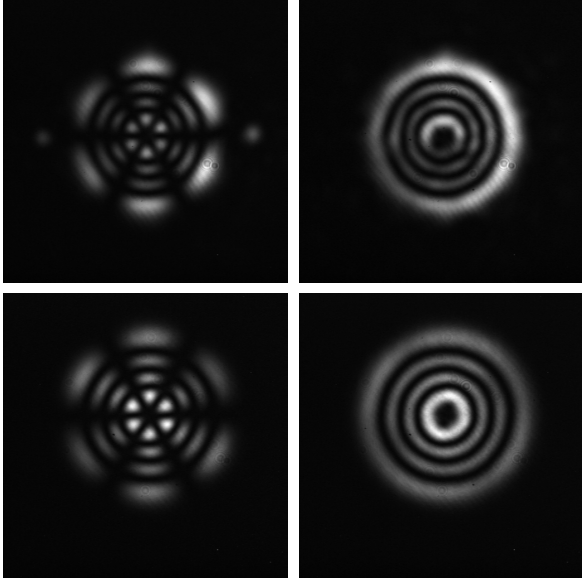


Figure 3: The measured intensity patterns of the sinusoidal (left column) and helical (right column)  $LG_{33}$  beams before (upper row) and after (lower row) transmission through the linear mode cleaner. The increase in mode purity upon transmission is already evident in the increased symmetry. The remaining asymmetry apparently is a result of the inaccuracy in the manual alignment of the input beam to the mode cleaner. This effect is the same for both images but more visually apparent in the case of the helical mode.

the residuals is less for the output  $LG_{33}$  beam than for the input beam. The residual of the transmitted beam also indicates that the mode deformation is dominated by a misalignment of the injected beam into the mode cleaner. Using this information, it was possible to create a beam pattern like the measured pattern using the interferometer simulation Finesse [16], when the model included an input beam misaligned by  $\alpha_x = -100 \mu\text{rad}$  in the horizontal plane, and  $\alpha_y = 60 \mu\text{rad}$  in the vertical plane. The residual pattern between the intensity pattern calculated with the Finesse simulation, and an ideal  $LG_{33}$  mode is shown in the right hand panel of figure 4. Based on the Finesse result we were able to produce a very good numerical model of the transmitted field amplitude and estimate the mode content by separately evaluating the overlap integrals between the complex field amplitude of the model and the field amplitudes of all LG eigenmodes. The results for the sinusoidal beam are shown in table II. Our model predicts that 99% of the light power is in the  $LG_{33}$  mode and most of the remaining light power is distributed in other modes of the order 9. A similar analysis for the helical mode gave effectively the same results for the mode purity.

Since the transmitted beam was to 99% in a single mode we were able to make an accurate estimate of the input mode purity by comparing the throughput of the  $LG_{33}$  modes to that of the  $LG_{00}$  mode. Once the intrinsic

$u_{lp}^{\text{sin}}$ mode	3, 3	4, -1	2, -5	4, 1	2, 5	other
power	99%	0.4%	0.3%	0.1%	0.1%	< 10 ppm

Table II: Mode decomposition of the numerical model of the sinusoidal  $LG_{33}$  beam transmitted through the linear mode cleaner, under an input beam misalignment of  $-100 \mu\text{rad}$  in the horizontal axis, and  $60 \mu\text{rad}$  in the vertical axis. The majority of the beam power is in the desired sinusoidal  $LG_{33}$  mode, with the rest almost entirely concentrated in other modes of order 9.

sic optical losses of the mode cleaner cavity were taken into account, we estimated the input mode purity to be 51% for the sinusoidal  $LG_{33}$  beam, and 66% for the helical  $LG_{33}$  beam. It should be noted that examples of higher-order LG modes with mode purity above 70% have undoubtedly been created previously directly with SLMs using a more thoroughly optimized conversion procedure, for example in [10], although in this case the authors refrain from quoting an experimentally measured purity. However, we believe this is the first time a purity improvement of a Laguerre-Gauss mode using an optical resonator to an estimated 99% has been demonstrated. The demonstrated mode purity is limited in first order by the manual alignment of the input beam and can very likely be improved using a standard automatic alignment system.

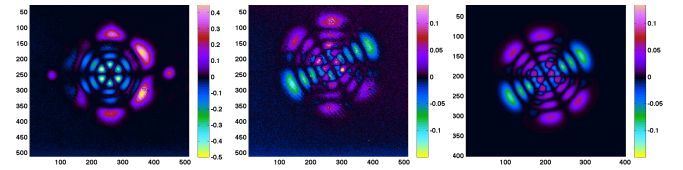


Figure 4: Residuals from best fits between intensity patterns and a theoretically ideal sinusoidal  $LG_{33}$  pattern. From left to right: the residual for the measured input  $LG_{33}$  beam, the residual for the measured output  $LG_{33}$  beam, the residual for an output  $LG_{33}$  pattern generated with a numerical model including a misalignment of the input beam to the cavity.

## B. Helical LG mode performance in a triangular mode cleaner

Triangular cavities behave differently from linear cavities in several ways. One important difference is that after one full round-trip in a triangular cavity any beam is mirrored about the vertical axis, which means that only light fields with symmetry about this axis can constructively interfere and be fully resonant. The intensity patterns of  $LG_{33}$  modes are symmetric regarding a mirroring around the vertical axis. However, the phase cross sections in general are not, as is shown in figure 5. Both types of sinusoidal modes show the required sym-

metry about the vertical axis, but helical modes do not. The anti-symmetric sinusoidal mode will be resonant in a cavity with an optical path length difference of  $\lambda/2$  from one resonant for the symmetric mode. In other words, a cavity tuned to be resonant for one type will be anti-resonant for the other. Furthermore any helical LG mode can be understood to be a sum of two sinusoidal LG modes, by considering equations 1 and 2 and the identity  $\exp(ix) = \cos(x) + i \sin(x)$ . We thus expect that in the case of a helical LG input beam, the mode cleaner cavity can be tuned to a length at which one of the constituent sinusoidal LG modes will be resonant and thus transmitted while the other constituent sinusoidal LG mode will be exactly anti-resonant and thus reflected, i.e. the helical LG beam would be decomposed into the two constituent sinusoidal modes.



Figure 5: Transverse phase distributions of the helical (left), vertically symmetric sinusoidal (center) and vertically anti-symmetric sinusoidal (right)  $LG_{33}$  modes. The color represents the phase, in a range from 0 (white) to  $2\pi$  (black).

In order to test this effect we placed a cavity of the standard triangular pre-mode cleaner design [18] after the linear mode cleaner as shown in figure 6. The triangular mode cleaner was scanned with the sinusoidal  $LG_{33}$  beam input and the helical  $LG_{33}$  beam input successively. As expected, extra resonances at half a free-spectral range were observed when the input was changed from sinusoidal  $LG_{33}$  to helical  $LG_{33}$ . The triangular mode cleaner was then feedback controlled in similar fashion to the linear mode cleaner, with the PDH error signal being this time obtained from the light reflected from the cavity input mirror. Figure 6 shows images of the input, transmitted and reflected beams at one of these resonances (the beam after the linear cavity was of slightly lower quality than that shown in figure 3 as less time was spent on the alignment optimization for this experiment). We observed that the beam transmitted through the triangular cavity was nearly a vertically symmetric sinusoidal  $LG_{33}$  mode. The stronger vertical central section compared to the one shown in figure 3 is due to astigmatism due to the curved end mirror [14]. The reflected beam was a superposition of all the modes rejected by the mode cleaner, and was therefore of lower mode purity than the transmitted mode. However, the vertically anti-symmetric  $LG_{33}$  mode can be seen to be the dominant mode present in the reflected light. The measurement was repeated for the alternative resonance point, where as expected the dominant type of the transmitted and

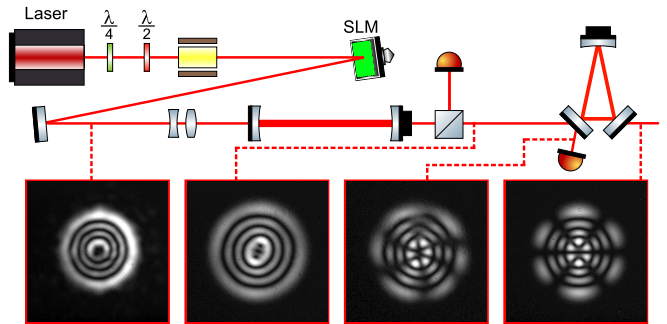


Figure 6: The experimental setup for transmitting a helical  $LG_{33}$  mode through a triangular mode cleaner, showing the intensity pattern of the beams at various locations in the setup (note that the images shown here are contrast enhanced to show the pattern more clearly). From left to right: helical  $LG_{33}$  after the SLM, helical  $LG_{33}$  after transmission through the linear mode cleaner, beam reflected from the triangular cavity and beam transmitted through the triangular cavity.

reflected mode was reversed. The helical input beam is decomposed into the constituent sinusoidal modes upon interaction with the triangular mode cleaner. We therefore conclude that in order for helical  $LG_{33}$  modes to be compatible with gravitational wave interferometers, the mode cleaners used must be linear, or at least be comprised of an even number of mirrors.

#### IV. CONCLUSION

Research into the interferometric performance of LG modes is important for the gravitational wave community, as LG modes offer a thermal noise advantage over the fundamental  $LG_{00}$  mode that can improve the sensitivity achievable by future detectors [1]. Simulations have already shown promising results for the interferometric performance of LG modes [3]. This article provides experimental verification for some of these predictions: We have demonstrated the generation of a PDH error signal from a linear mode cleaner injected with both helical and sinusoidal  $LG_{33}$  modes equivalent to the error signal obtained with a  $LG_{00}$  mode. We used this error signal to successfully demonstrate longitudinal control of the linear mode cleaner cavity at resonance for the  $LG_{33}$  mode; a vital technique for the operation of gravitational wave interferometers with  $LG_{33}$  modes. We also showed an increase in the purity of a sinusoidal  $LG_{33}$  mode from 51% to 99% upon transmission through a linear mode cleaner, demonstrating that very high-purity  $LG_{33}$  mode light sources can be produced in this way. Furthermore, we have demonstrated the decomposition of a helical  $LG_{33}$  mode into the constituent sinusoidal  $LG_{33}$  modes with a triangular mode cleaner; a result which has a strong impact on the choice of the optical design of future detectors.

The prospects for LG modes in gravitational wave

detectors remain intact following the investigation described in this paper. In the future we will expand this work to use LG modes in systems that combine Michelson interferometers and resonant cavities, and also include alignment control systems. The requirements for mirror surfaces for high finesse systems with LG modes also needs further investigation to move scrutiny of the interferometric performance of LG modes to the next level, towards a possible implementation in future gravitational wave detectors.

## V. ACKNOWLEDGMENTS

We would like to thank M. Padgett and the optics group from Glasgow University for their assistance and

advice. We would also like to thank J. Nelson from the Institute for Gravitational Research for his support with the SLM. This work has been supported by the Science and Technology Facilities Council and the European Commission (FP7 Grant Agreement 211743). This document has been assigned the LIGO Laboratory document number LIGO-P1000040

- 
- [1] B. Mours, E. Tournefier, and J.-Y. Vinet, *Classical and Quantum Gravity* **23**, 5777 (2006).
  - [2] J.-Y. Vinet, *Living Reviews in Relativity* **12** (2009), URL <http://www.livingreviews.org/lrr-2009-5>.
  - [3] S. Chelkowski, S. Hild, and A. Freise, *Physical Review D (Particles, Fields, Gravitation, and Cosmology)* **79**, 122002 (pages 11) (2009), URL <http://link.aps.org/abstract/PRD/v79/e122002>.
  - [4] A. Siegman, *Lasers* (University Science Books, 1986).
  - [5] G. A. Turnbull, D. A. Robertson, G. M. Smith, L. Allen, and M. J. Padgett, *Optics Communications* **127**, 183 (1996).
  - [6] J. Courtial and M. J. Padgett, *Optics Communications* **159**, 13 (1999).
  - [7] S. A. Kennedy, M. J. Szabo, H. Teslow, J. Z. Porterfield, and E. R. Abraham, *Phys. Rev. A* **66**, 043801 (2002).
  - [8] A. Freise and K. Strain, *Living Reviews in Relativity* **13**, 1 (2010), URL <http://relativity.livingreviews.org/Articles/lrr-2010-1/>.
  - [9] J. Arlt, K. Dholakia, L. Allen, and M. J. Padgett, *Journal of Modern Optics* **45**, 1231 (1998).
  - [10] N. Matsumoto, T. Ando, T. Inoue, Y. Ohtake, N. Fukuchi, and T. Hara, *Journal of the Optical Society of America A* **25**, 1642 (2008).
  - [11] A. Rüdiger, R. Schilling, L. Schnupp, W. Winkler, H. Billing, and K. Maischberger, *Optica Acta* **28**, 641 (1981).
  - [12] S. Goßler, M. M. Casey, A. Freise, A. Grant, H. Grote, G. Heinzel, M. Heurs, M. E. Husman, K. Kötter, V. Leonhardt, et al., *Review of Scientific Instruments* **74**, 3787 (2003).
  - [13] A. Genin, J. Marque, B. Swinkels, and G. Vajente, *Tech. Rep. VIR-0232A-10*, Virgo (2010).
  - [14] paper in preparation.
  - [15] E. D. Black, *Am. J. Phys.* **69**, 79 (2000).
  - [16] A. Freise, G. Heinzel, H. Lück, R. Schilling, B. Willke, and K. Danzmann, *Classical and Quantum Gravity* **21**, S1067 (2004), software available at: <http://www.gwoptics.org/finesse>.
  - [17] P. Kwee, F. Seifert, B. Willke, and K. Danzmann, *Review of Scientific Instruments* **78**, 073103 (2007).
  - [18] B. Willke, N. Uehara, E. K. Gustafson, R. L. Byer, P. J. King, S. U. Seel, and J. R. L. Savage, *Opt. Lett.* **23**, 1704 (1998).